Astron. Astrophys. 284, 801–809 (1994)

ASTRONOMY
AND
ASTROPHYSICS

Morphological segregation of galaxies in clusters

I. The non-uniform distribution of types in the inner region of Perseus *

Stefano Andreon

Observatoire Midi-Pyrénées, Unité Associée au CNRS n. 285, 14, Avenue Edouard Belin, F-31400 Toulouse, France

Received 7 July 1993 / Accepted 2 November 1993

Abstract. A Monte Carlo method for measuring the significance of possible space, velocity and/or luminosity segregation among galaxies of different Hubble types is presented. It relies on five statistical tests. This method is applied to a sample of early-type galaxies with reliable morphological classifications in the inner region of the Perseus cluster. A strong spatial segregation is detected: ellipticals are displaced eastward with respect to the cluster center, lenticulars northward, barred lenticulars southward, while disky ellipticals occupy the whole inner region of the cluster. This non-uniform distribution of morphological types is interpreted as an indication that the Perseus cluster, although claimed relaxed, is in reality not virialized and dynamically young. No statistically significant morphology-density or morphology-radius relations are detected showing that the primary source of the morphological segregation in this cluster is tied to the non-uniform spatial distribution of Hubble types and not to the local density or the distance from the cluster center. The number of spirals in the inner region of Perseus is underestimated in the literature by a factor 2 or 3. Finally, the bright ends of the luminosity functions of boxy and disky ellipticals do not differ statistically.

Key words: galaxies: cluster: Perseus cluster – elliptical and lenticular – spiral – fundamental parameters – formation – interactions – luminosity function

1. Introduction

Many physical properties of elliptical galaxies are correlated with the deviations of isophotes from a perfectly elliptical shape: radio, X-ray and kinematical behavior (Bender 1988a; Bender et al. 1989; Nieto & Bender 1989), UV emission (Longo et al. 1989), optical luminosity and mass (Nieto & Bender 1989; Nieto et al. 1993), three-dimensional shape (Bender 1988b; Nieto 1988; Fasano 1991; Nieto et al. 1993), and central luminosity profiles (Nieto et al. 1991).

It is believed that the dichotomy of ellipticals into two classes is tied to different evolutionary histories (Bender et al. 1989; Nieto & Bender 1989): disky ellipticals are, as S0s, galaxies whose structure has hardly been affected by interactions, whereas the boxiness of boxy ellipticals is the results of merging or of accretion of material onto the galaxy. Alternative explanations exist however, see Schweizer et al. (1990).

An environmental study of early-type galaxies should provide some insight into the recent past of these objects because of the fundamental role played by the environment in determining the galaxy morphological type (Dressler 1980), in producing morphological disturbances (Lauer 1988; Schweizer et al. 1990), in modifying the surface brightness profile of galaxies (Ostriker & Hausman 1977; Kormendy 1977) and in determining the radio emission (Vettolani & Gregorini 1988).

For such a study, it is necessary to have a large sample of galaxies classified in high resolution conditions, in order to discriminate between disky and boxy ellipticals, but also between Es and S0s if the cluster is as far or further than Perseus, since already at that distance about 40-50% of early-type galaxies are misclassified (see Sect. 6).

Large samples of early-type galaxies in different environments have been collected by our team in the past four years: early-type type galaxies of the Shapley-Ames catalogue (Nieto et al. 1992), paired ellipticals (Contini et al. in preparation), elongated ellipticals (Nieto et al. 1991; Nieto et al. 1993) and complete samples of galaxies in the Perseus and Coma clusters (works in progress).

In this paper we present the method utilized for such an environmental study and we apply it to the inner region of Perseus using the data collected by Poulain et al. (1991, hereafter PND). Future papers will present the results for the outer region of Perseus and for the Coma cluster.

* Based on observations made with the 2m telescope of Pic du Midi Observatory, operated by INSU (CNRS), with the Canada-France-Hawaii Telescope, operated by the National Research Council of Canada, the Centre National de la Richerche Scientifique of France and the University of Hawaii, USA and with the Schmidt telescope at the Calern Observatory (OCA)

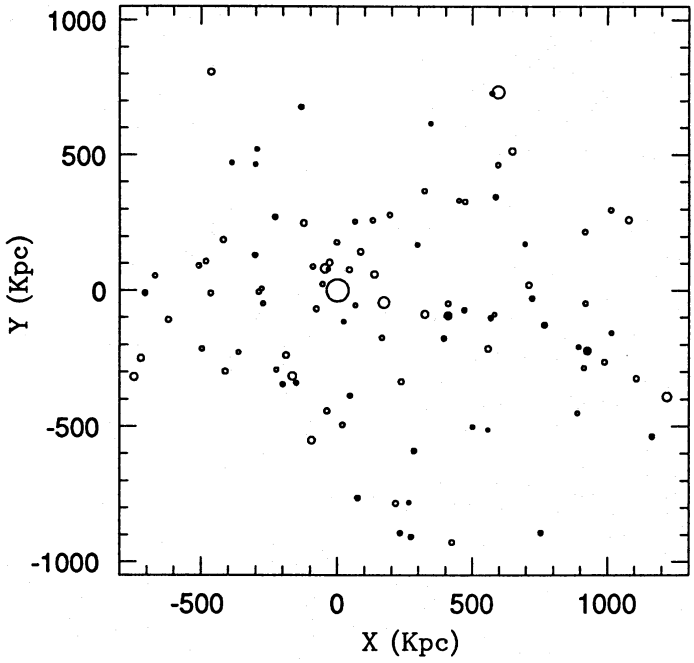

Fig. 1. Space distribution of the classified (open circles) and unclassified (filled circles) galaxies in the inner region of the Perseus cluster. North is up and East is left. Larger circles mark brighter galaxies

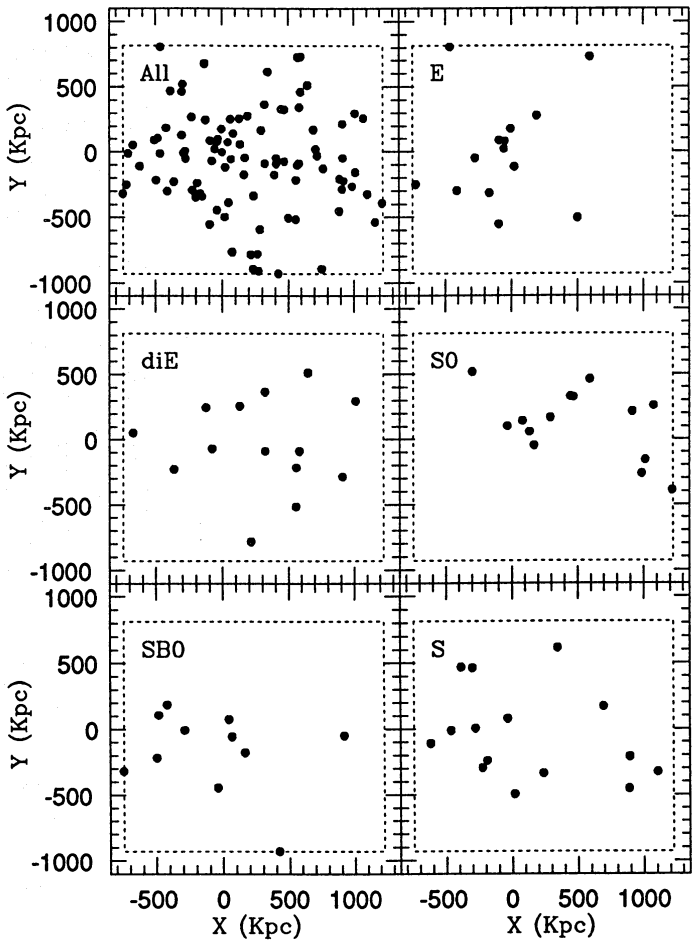

Fig. 2. Space distribution of all the galaxies of Perseus and of each morphological type

2. The sample

Optically, the Perseus cluster of galaxies (Abell 426) is of Bautz-Morgan (1970) type II-III, i.e. intermediate in the relative contrast of the brightest cluster galaxy to other galaxies in the cluster. The prominent chain of luminous galaxies, for which the cluster is classified of Sastry-Rood type L (Bahcall 1974), is roughly extended in a direction which forms a 15 degree angle with the E-W direction (Bahcall 1974, see also Fig. 1). The center of the distribution of galaxies is located to the West of NGC 1275, brightest galaxy in the cluster (Bahcall 1974). The Perseus cluster is spiral-poor and of high velocity dispersion (Melnick & Sargent 1977).

The sample used for the analysis of the inner region of Perseus is formed by a subsample of Bucknell et al. (1979) complete catalogue of galaxies in Perseus (hereafter BGP). The x, y positions of BGP galaxies have been transformed into α, δ coordinates by a linear interpolation between the x, y coordinates of the subsample of BGP galaxies having an identification (NGC or IC number) and the α, δ coordinates of the same objects given in PND. We have selected all the BGP galaxies brighter than blue magnitude 15.7 in the region $3^h13^m25^s < \alpha < 3^h18^m21^s$ and $40°53'16" < \delta < 41°42'50"$. The reason for this choice is to minimize the number of galaxies for which no high-resolution images have been obtained, or, in other words, to maximize the number of galaxies of known morphology.

Radial velocities were taken from the Catalogue of Principal Galaxies (Paturel et al. 1989). The resulting sample contains 96 galaxies, of which 8 have no measured radial velocity and 29 are not observed in PND. From visual inspection of a Palomar sky survey print and a Schmidt 4415 hypersensitized plate of the cluster, taken at the Calern Observatory in December 1992, 8 of the galaxies not observed by PND show spiral arms and thus are spiral galaxies. The galaxies with detailed morphological classification represent 78% of the total sample. A radial velocity is available for all the galaxies observed in high-resolution conditions.

The morphological classification was taken from PND who obtained it by a quantitative analysis of the isophote shape and surface brightness profile of their galaxies. When the morphology quoted there is intermediate between two Hubble types we choose the earlier classification to be conservative. To avoid any risk of misclassification, all the other galaxies, except those with obvious spiral arms, were rejected from the sample, even if the type is available in the literature. To give an example of misclassification, the galaxy CR13 has been classified spiral by Baggett & Anderson (1992), lenticular by Kent & Sargent (1983), but turns out to be a disky elliptical when observed in good seeing conditions (PND). On the other hand, our procedure for classifying spiral galaxies, based on the presence of spiral arms, avoids any possibility of misclassification.

It is important to note that the majority of the 29 galaxies not observed in high-resolution conditions are classified spirals in the literature (this is the very reason why they were not observed by PND). As a consequence, the quoted percentage of

completeness for early-type galaxies, 78%, is a lower limit. The sample of early-type galaxies is in fact almost complete.

There are 14 ellipticals, disky ellipticals (diEs) and S0s, 11 SB0s and 18 Ss in our subsample, and, for the above reason, the fraction of spirals is certainly underestimated.

Figure 1 shows the positions of the galaxies in the adopted region of study. The region is centered on the chain of bright galaxies of Perseus and covers an area of 1 square degree. Figure 2 shows the positions for the whole subsample and for each Hubble type separately; the region under study is delimited by a dotted line in this figure. Each Hubble type obviously occupies a specific region of the cluster: ellipticals populate preferentially the Eastern part of the cluster and avoid the region occupied by lenticulars which stay preferentially in the North-Western corner; barred lenticulars appear to be located rather in the South-East. Finally, disky ellipticals occupy the whole region. A morphological segregation is thus obviously present in this cluster.

3. Monte Carlo simulations

To test the reality of the segregation that appears in Fig. 2 and, if real, to understand if it is the result of the morphology-density or the morphology-radial distance from the cluster center relations, we compute the probability that such a segregation is the result of chance and we explore also the possibility that it arises from a density or a radial segregation. The same analysis is also conducted for the velocity and luminosity axes.

3.1. Tests for morphological segregation

Five statistical tests were performed to provide a quantitative description of the presence and significance of morphological segregations in Perseus. We have computed the following statistical quantities that are sensitive to the existence of a morphological segregation : the position of the galaxies in the plane of the sky have been computed in polar coordinates (r, θ) centered on NGC 1275 and in a Cartesian coordinate system (x,y) rotated by 15 degrees clockwise with respect to (α, δ), so that the abscissa is along the chain of bright galaxies of the cluster. Then, for each pair of Hubble types, the distributions of the galaxies along the x, y, r and θ axes have been compared. The same analysis has been conducted with the distributions along the velocity, density and luminosity axes in order to look for a morphological segregation along these axes. The density is defined as in Dressler (1980).

Finally, since it appears in Fig. 2 that the galaxies of one Hubble type avoid the region occupied by the galaxies of other types, the distances of each galaxy to the nearest galaxies of similar and of different Hubble type have been computed and compared. If galaxies of two different Hubble types avoid each other, the two distributions will clearly be different.

3.2. Description of the statistical tests

i) T test

For each pair of distributions we compute t, the absolute value of the difference between the means of the two distributions divided by the pooled variance of the two distributions; this statistical quantity is the one used in the T test. When applied to the x, y, θ coordinates, it quantifies the probability that galaxies of different Hubble types have different centers. When applied to the r coordinate it quantifies the presence of the usual radial morphology segregation.

ii) K-S test

For each pair of distributions we compute d, the maximum value of the absolute difference between the two cumulative distributions after having normalized the range of each distribution from 0 to 1. This statistical quantity is the one used in the Kolmogorov-Smirnov test. This test quantifies the presence of a difference in the distribution without providing any information about the way in which the two distributions differ, but it can detect differences not detected by the other tests.

iii) F test

For each couple of distributions we compute f, the maximum of rd and $1/rd$, where rd is the ratio of the dispersions of the two distributions. This statistical quantity is the one used in the F test. This test, when applied to the x, y, θ coordinates, quantifies the probability that different Hubble types have a different degree of spatial concentration. When applied to the r coordinate it quantifies the presence of the usual radial morphology segregation.

iv) TI test

For each couple of distributions we compute ti, the maximum of rti and $1/rti$, where rti is the ratio of the tail indices of the two distributions, the latter defined (Beers et al. 1991) as

$$tail\ index = (q(90) - q(10))/(q(75) - q(25))$$

where $q(x)$ is the x percentile.

This test quantifies the presence of wings of different importance in the two distributions.

v) SI test

For each couple of distributions we compute si, the maximum of rsi and $1/rsi$, where rsi is the ratio of the skewness indices of the two distributions, the latter defined by analogy with the tail index as

$$skewness\ index = (q(50) - q(10))/(q(90) - q(50))$$

This test measures the probability that the two distributions have a different skewness.

The form of the latter two statistics is chosen by analogy with the F test since the statistics defined by f, ti and si are two tailed distributions, either very large or very small values indicating very significant differences.

We point out that all these statistics for measuring differences in the distributions are not simply redundant ways of measuring the same property, since each test is sensitive to a different aspect of possible differences between the distributions. These statistics are in fact complementary measures.

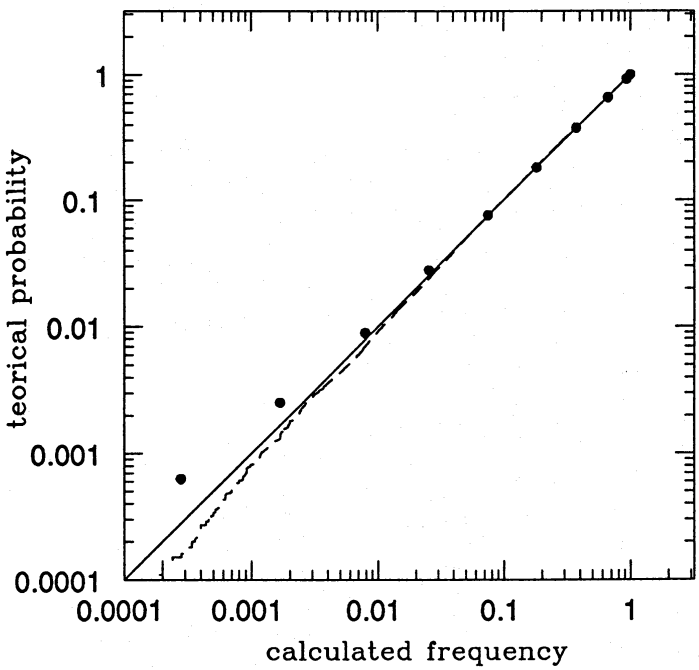

Fig. 3. Theoretical probability vs calculated frequency in the tests of our simulations. The straight line represents the case in which the two probabilities are equal, the dotted line represents the results found for the T test, whereas the points are the results of the K-S test

Finally, we also considered the statistical quantities formed by the vectors (T, F, KS), (T, F, KS, TI) and (T, F, KS, TI, SI) whose probabilities are named P3, P4 and P5 respectively.

3.3. Implementation of the morphological tests

It is important to verify that the differences found with these statistical tests are real and that the latter do not simply detect random fluctuations. These tests are thus calibrated on a set of artificial clusters with no morphological segregation, generated by a Monte Carlo technique.

In order to guarantee that the distributions (in position, velocity, etc.) of all galaxies in the artificial clusters, regardless of morphological type, are equal to those of the real one, the real cluster itself was used to simulate the artificial clusters. Artificial clusters with no morphological segregation were generated by assigning randomly a Hubble type to the galaxies. 50000 of these clusters were generated for each comparison of Hubble types distributions.

In the artificial cluster, the galaxies of the different morphological classes are selected in the following way. We first generate a series of integer random numbers, as many as there are galaxies in the sample, and, since the galaxies of the sample are numbered, each random number will enable us to select one galaxy. The random numbers should all be different, otherwise we would select twice (or more) the same galaxy.

Each probability is then computed as the fraction of artificial clusters with a statistical quantity larger than the one measured in the real cluster. These probabilities are thus equivalent to frequencies.

3.4. Check of the morphological tests

It is essential for the correctness of the tests that the frequencies calculated by Monte Carlo technique do not differ from the theoretical probabilities, e.g. by the use of a poor random number generator. Thus the tests must be checked in the exact experimental conditions, namely the generation of unequal random integers.

For this reason, we have to compare the frequencies calculated by Monte Carlo technique with the theoretical ones in a case where we know the theoretical probability function which has to be for integer random numbers of uniform probability. The two theoretical probability functions that we know satisfying the conditions are the T and K-S tests; the F-test cannot be used, because it does not concern uniform distributions.

For the check itself, we set the number of objects in each morphological class at 15, which is the typical number of galaxies for each morphological class in the real cluster, whereas the number of Monte Carlo simulations is 50000 as in all simulations of artificial clusters.

The calculated frequency functions for the T and K-S test are presented in Fig. 3 as a function of the theoretical ones (shot-dashed lines, and filled points respectively)*. The solid line represents the case when the theoretical probabilities are equal to the Monte Carlo frequencies. For both tests, the agreement between the calculated frequency function and the theoretical probability is good over all four decades in probabilities given in the figure, the absolute difference being in the range 1 to 3/10000, a quantity that can be completely accounted for by poissonian noise due to the limited number of simulations and that in any case for our purpose is negligible since it does not change significantly the absolute value of the probabilities. There are thus no significant systematic errors in our simulations. The simulations also show that the poissonian noise, due to the limited number of simulations (50000) is as low as expected.

4. Results of the tests

Table 1 shows the probability, expressed in percentage, that each pair of Hubble types has the same parental x, y, radial, angular, velocity, density, nearest-galaxy and luminosity distributions. Small values indicate different parental distributions. Columns 1 and 2 list the pair of Hubble types and the axes considered respectively. Columns 3, 4, 5, 6, and 7 list the results for the T, F, TI, SI, KS test respectively. Columns 8, 9 and 10 list the probabilities P3, P4 and P5 respectively. For the sake of clarity only pairs of Hubble types showing differences with a proba-

* The frequency and probability functions for the K-S test are correctly discrete since each distribution is composed of a finite number of elements: consequently the absolute difference between the two cumulative distributions and their associated probabilities can take a number of values at most equal to the number of elements in each class.

Table 1. Probabilities, expressed in percentage, that each pair of Hubble types has the same x, y, radial, angular, nearest-galaxy, velocity, density & luminosity distributions. Only pairs of Hubble types showing differences with a probability P5 larger than 99,9 % are listed.

pairs of Hubble types (1)	axes (2)	T (3)	F (4)	TI (5)	SI (6)	KS (7)	P3 (8)	P4 (9)	P5 (10)
Es vs diEs	x	2.962				1.790	0.262	0.090	0.060
Es vs S0s	x	0.278		10.072		0.112	0.032	0.004	0.004
Es vs S0s	y	4.780	1.456			1.532	0.024	0.018	0.018
Es vs Ss	x		9.052		3.564		2.490	0.242	0.032
diEs vs S0s	y	7.560	7.438			1.872	0.162	0.050	0.004
diEs vs S0s	near	0.074		9.814		0.016	0.008	0.008	0.004
diEs vs Ss	near	0.642				1.236	0.170	0.160	0.040
S0s vs SB0s	y	0.024			1.728	0.254	0.010	0.002	0.000
SB0s vs Ss	y	10.200			4.238		8.890	2.888	0.012
SB0s vs Ss	L	7.584		3.684		7.598	1.182	0.112	0.016

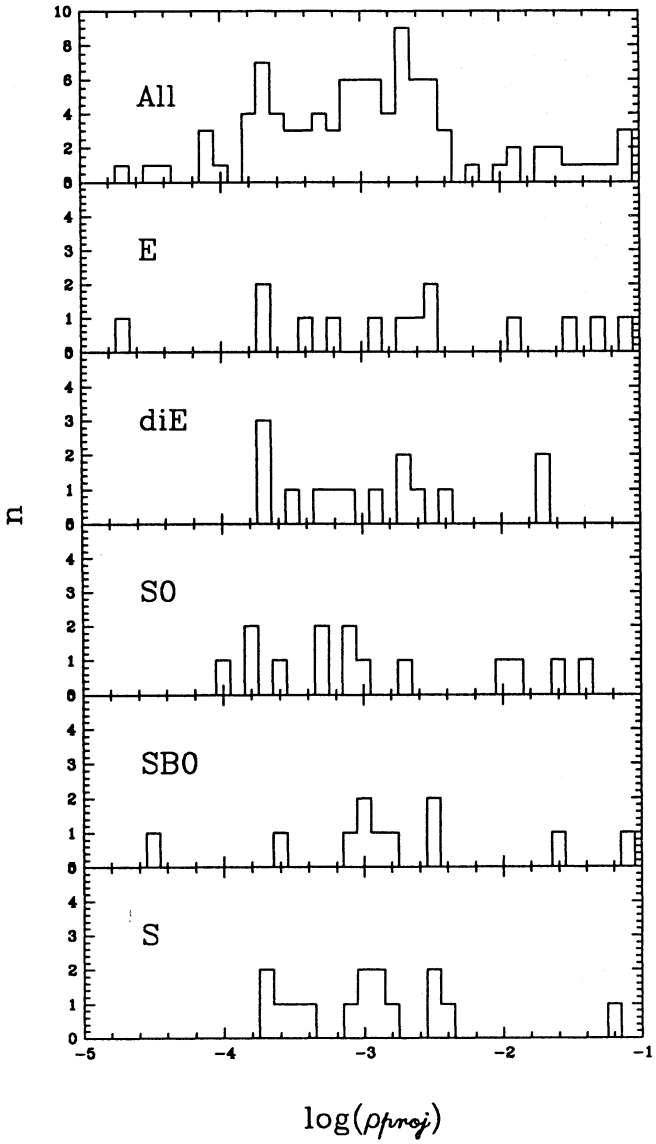

Fig. 4. Histogram of the distribution in density space of all galaxies and of each morphological Hubble type separately

bility P5 larger than 99,9 % are listed. Null detections are not listed but they are discussed in Sect. 6.

The principal detected differences are the following:

– *Es vs diEs*

The two Hubble types have different x distributions (P4 and P5 are less than 10^{-3}) due to an Eastward displacement of the center of the ellipticals' distribution compared to that of disky ellipticals (T = 3.0%, see also Fig. 2) and a global difference between the distributions (KS = 1.8%).

– *Es vs S0s*

The two Hubble types have different distributions in the x and y directions (P4 and P5 equal to $4 * 10^{-5}$ and $1.8 * 10^{-4}$ respectively for both x and y); the center of the ellipticals' distribution is displaced Eastward ($T = 2.8 * 10^{-3}$, see also Fig. 2) and they have a marginally larger dispersion in the y direction (F=1.5%) combined with a marginal Northward displacement (T=4.8%).

– *Es vs Ss*

The x distributions of the two Hubble types differ ($P5 = 3.2 * 10^{-4}$) because of the different skewness of the two distributions (SI = 3.6%) and the larger dispersion of the ellipticals' distribution (F = 9%; see also Fig. 2).

– *diEs vs S0s*

The y distributions of the two Hubble types differ ($P4 = 5 * 10^{-4}$, $P5 = 4 * 10^{-5}$) because the lenticulars' distribution is marginally Northward displaced (T = 7.4%), it has a marginally larger dispersion (F = 7.5%), and because of a global difference between the two distributions (KS= 1.9 %).

The nearest-galaxy distributions of the two Hubble types are clearly different (P3, P4 and P5 less than 10^{-4}) because, for disky ellipticals, the nearest galaxy of same Hubble type is farther that the nearest lenticular (T = 0.07%; see also Figure 2).

– *diEs vs Ss*

The nearest-galaxy distributions of the two Hubble types differ ($P5 = 4 * 10^{-4}$) because disky ellipticals avoid each other more than spirals (T = 0.6%; see Fig. 2).

– *S0s vs SB0s*

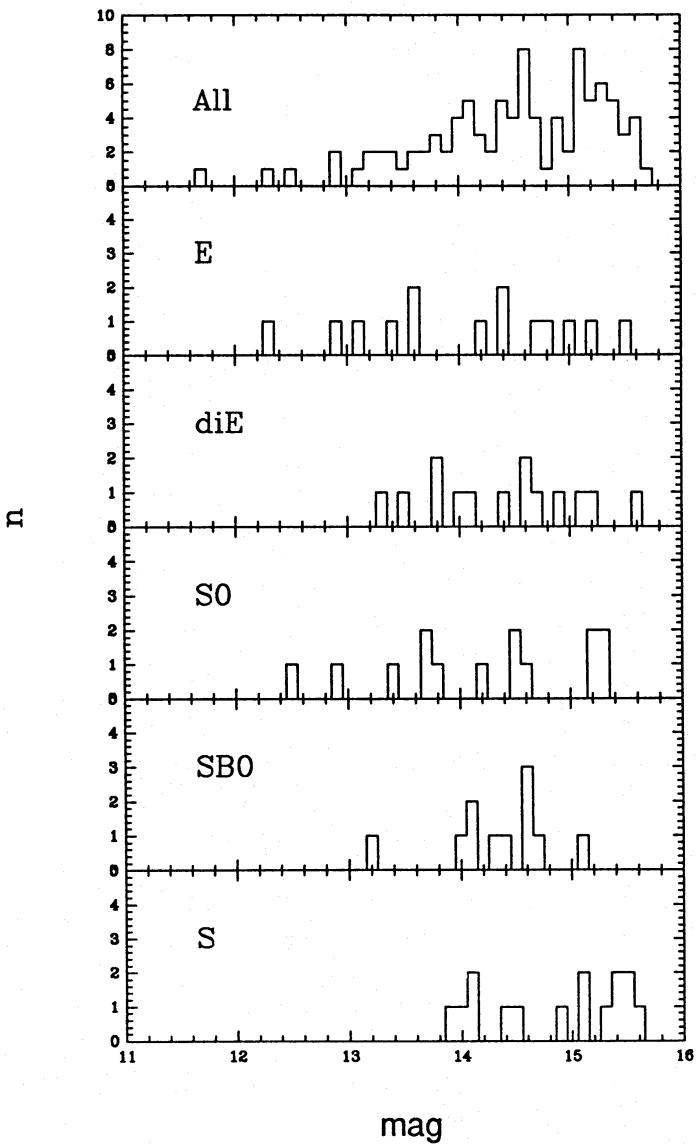

Fig. 5. Histogram of the luminosity distribution of all galaxies and of each morphological type separately

The y distributions of the two Hubble types are clearly different (P4 and P5 less or of the order of 1/50000) because of the Northward displacement of the lenticulars' distribution (T = 0.02%).

– *SB0s vs Ss*

The y distributions of the two Hubble types differ (P5 = 0.01%) because of the absence of the North tail of the SB0s distribution (SI= 4.2%, see also Fig. 2).

The luminosity distributions of SB0s and Ss are different (P5=0.016%) because the Ss' luminosity distribution has larger tails (TI=3.7%) and a marginally lower mean (T=7.5%) (see also Fig. 5).

5. Completeness and sampling

We determined the spatial and velocity distributions of galaxies in Perseus from an observed subsample. In statistical theories,

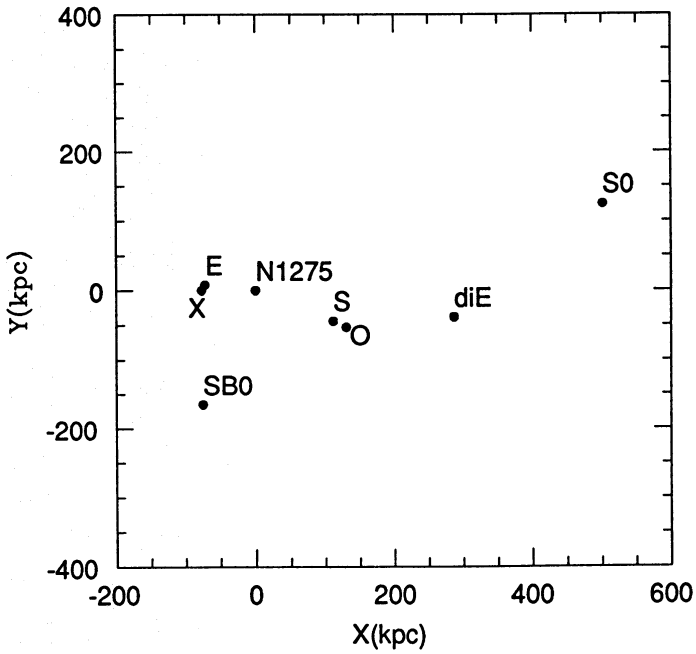

Fig. 6. Centers of galaxy distributions in the inner region of the Perseus cluster. The optical center is marked by an O and the X ray-centroid with an X. North is up and East is left

if the subsample is chosen randomly, it possesses the properties of the whole sample so that, from this point of view, its incompleteness is unimportant. The sampling is defined as random if there is no connection between the method of selection and the properties under consideration (Kendall & Stuart 1948). In our case this means that the selection criteria of different Hubble types must not differ. We have several reasons to believe that this is the case for early-type galaxies.

First of all, the spatial and nearest-galaxy distributions of galaxies of different Hubble types differ in many aspects tied to different moments of their distributions; it is difficult to find a selection criterion able to produce all these differences.

Secondly, we have no reason to think that the selection criteria for different Hubble types differ. Indeed, the galaxies observed by PND were selected from the Kent & Sargent (1983) sample among the ones that are not classified spirals in the literature. There was no other particular preference to choose the galaxies to observe. Also, any choice done before or during the observations cannot introduce different selection criteria for the different Hubble types because the Hubble type of the galaxies is unknown at that time. All observed galaxies were analyzed, so no choice was done after the observations.

Finally, the completeness of the subsample of observed galaxies is high, 78%, and, as already explained, the majority of the unobserved galaxies are classified as spirals in the literature and consequently the completeness for early-type galaxies is higher. Obviously, the high completeness strongly limits the effect of any selection criteria.

For these reasons we think that the subsample of observed early-type galaxies is representative of the whole sample of early-type galaxies, in the inner region of the cluster, brighter

than 15.7 mag and that the remaining incompleteness has little effect on the analysis.

The galaxies of the Perseus cluster were observed during different observing runs and from different observatories (see PND for details). We have verified that galaxies of equal morphological type are not observed preferably during the same run or at the same observatory, in which case the classification might be biased by some run dependent effect (seeing conditions, telescope optical configuration, etc.).

The almost completeness of the sample also allows us to compare the space, density, nearest-galaxy and velocity distributions of spirals to the early-type ones even if the selection criteria for spirals differs from those for the early-type galaxies. To make sure that the 22% unclassified galaxies do not change our results, the probabilities of all tests involving spirals have been re-computed using as spiral sample the 16 spirals of the studied region minus 3 chosen randomly. No new morphological segregation appears or disappears when we subtract this subsample that represents 19% of all the galaxies classified as spirals, showing that the remaining incompleteness of the sample (22%) is probably unimportant.

6. Discussion

6.1. Summary of the results

- The inner region of Perseus presents a strongly non-uniform distribution of morphological types; this means that the general appearance of the cluster in space depends on the observed Hubble type. More precisely, as visible in Figs. 2 and 6, the ellipticals' spatial distribution has the same center as the X-ray emission of the cluster, and is Eastward displaced along the cluster's chain of bright galaxies compared to all but the SB0s' spatial distributions. Again, the spatial distribution of S0s is Northward displaced compared the other ones. Finally the SB0s one is Southward displaced with respect to the Ss one. This non-uniform distribution of morphological types in the cluster is statistically significant at least at a level of 99,9 % (or $\sim 3\sigma$) and sometimes at a level of $\sim 99,998$ % (or $\sim 4\sigma$) as in the case of the displacement in the South-North direction of SB0s and S0s.
- No significant differences are found among the distributions of galaxies of different Hubble types in velocity space, contrary to what happens for the spatial distributions.
- A morphological anticoncordance, i.e. a trend for the galaxies of same Hubble type to avoid each other more than other Hubble types, is detected for galaxies with a disk: disky ellipticals avoid each other more than S0s and Ss.
- No significant differences are found among the distributions of galaxies of different Hubble types in the density and distance from the cluster center axes.
- No large differences are found between the luminosity distributions of all pairs of Hubble types, except Ss and SB0s. Spirals are fainter and have a distribution which covers a larger range in luminosity than SB0s (Fig. 5). The bright ends of the luminosity functions of boxy and disky ellipticals do not differ statistically, contrary to Bender at al.'s (1989) claim. Their sample is, however, biased by the presence of radio and X-ray loud galaxies, that tend to be boxy; removing those, the remaining sample is too small for deriving any statistically significant result.

Table 2. Comparison of morphological classification of early type galaxies at different resolutions. Each number show how many galaxies classified as y are, when observed in high resolution conditions, of type x

x \ y	E	S0
	n (%)	n (%)
E	15 (34%)	1 (3%)
diE	9 (20%)	2 (6%)
S0 & SB0	14 (32%)	23 (64%)
S	6 (13%)	10 (28%)
Total	44 (100%)	36 (100%)

6.2. Morphological classification of spiral galaxies

In their morphological study of the Perseus cluster, Melnick & Sargent (1977) found two spiral galaxies among the 65 brighter galaxies in a circular region of same area and center as our almost square region. When our classification is considered, there are in the studied region 6 spirals (and 14 unclassified galaxies, many of which are probably spirals) among the 65 brighter (classified and unclassified) galaxies or 12 spirals among the 65 brighter classified galaxies. Inspection of the space distribution of our spiral galaxies shows that there are not enough spiral galaxies outside the region studied by Melnick & Sargent and inside ours to account for the different estimates of the number of spiral galaxies. The larger number of galaxies classified as spirals by PND is simply a consequence of using high-resolution images and performing a quantitative analysis of the isophote shape and surface brightness profile of the galaxies.

Although the number of galaxies classified as spiral in the two works is rather small for computing the exact value of the ratio of the two spiral fractions, an indicative and cautious value could be ~ 3. Since the morphological classification is a more and more difficult tool as the distance of the galaxy to be classified increases, in all more distant clusters for which the spiral fraction is computed in the same way, i.e. from visual inspection of plates, the fraction of spirals is underestimated by at least the same amount. The dependence of the apparent spiral fraction of clusters on distance (Andreon 1993) confirms independently the underestimation of the true spiral fraction in nearby clusters.

6.3. Morphological classification of early-type galaxies

The effect of distance on the morphological classification has been quantified by Andreon (1993). Here we quantify the effect of the resolution and the quality of visual classifications. For the early-type galaxies in the Perseus cluster, we compare the

classification obtained by visual estimates on plates (collected from the literature as reported in PND) to the one obtained by isophotal shape analysis of high resolution CCD images by PND. To enlarge the sample, all galaxies of PND classified in the literature E or S0, independently of their luminosity or spatial position in the Perseus cluster, are retained here. Table 2 shows the results.

Of the whole sample of galaxies classified as S0 by visual estimate $\sim 1/4$ are Ss, $\sim 2/3$ are S0s, and $\sim 1/10$ are galaxies of earlier type (Es and diEs). Of the whole sample of galaxies classified as E by visual estimate $\sim 1/2$ are galaxies of type later than or equal to S0 and $\sim 1/5$ are diEs. So, just $\sim 1/3$ of galaxies classified E in the literature have no disk. Conversely, in the hypothesis that true Es and S0s are not misclassified Ss by visual estimate, true Es are almost always classified correctly, true Disky ellipticals are classified E and true S0s are classified correctly 2 times out of 3 and once E. Spirals, when not classified correctly, are classified E or S0 at almost the same rate.

A disturbing consequence of this misclassification is that a sample twice the necessary one has to be observed and analyzed in all studies of complete samples of Es (Disky + Boxy) or S0s, as ours.

6.4. The dynamical age of the Perseus cluster

As noted above, the Perseus cluster presents strong spatial non-uniformities in the distribution of morphological types[1]. This non-uniformity is, at first sight, similar to the one detected in the Virgo cluster (Binggeli et al. 1987), where the spatial distributions of Es and spirals are not co-centered. But in Virgo, as opposed to Perseus, the velocity distribution of Es differs from that of spirals. Also, the morphological non-uniformity detected in Virgo is compatible with the morphology-density relation whereas in Perseus it is not. No comparison between the two works can be done for the other Hubble types because the study of Virgo splits the galaxies in classes that differ from ours.

In a virialized cluster, one expects all initial non-uniformities to be smoothed out and/or deleted by the dynamical evolution of the cluster (West et al. 1993, but see, however White 1976 and Cavaliere et al. 1986). It is not surprising that the Virgo cluster is inhomogeneous since it is a dynamically young cluster (Sarazin 1986; Forman & Jones 1982). On the contrary, the inner region of the Perseus cluster, prototype of evolved and virialized clusters (Forman & Jones 1982; Sarazin 1986) should be uniform, contrary to observational evidence. The morphological non-uniformity thus suggests that the Perseus cluster is not completely virialized.

Two other facts independently suggest that the Perseus cluster is dynamically young.

The non coincidence of the optical and X-ray centers of the Perseus cluster has already been noted (Bahcall 1977; Branduardi-Raymont et al. 1981). Consequently the dark matter distribution is not co-centered with the visible one, reinforcing the idea that the bright matter of the Perseus cluster is at an early stage of its dynamical evolution.

NGC1275, the brightest galaxy, is not located at the center of the dark matter distribution (see Fig 6). If the Perseus cluster were not dynamically young, NGC1275 would be tidally limited to a radius of the order of 30 kpc (Merritt 1984) assuming a cluster core radius of the order of 250 kpc (Bahcall 1974; Branduardi-Raymont et al. 1981). The surface brightness profile of NGC 1275 does not show any tidal cut-off at radii less than 150 kpc (Oemler 1976) confirming again the early stage of dynamical evolution of the cluster. A smaller cluster core radius, as suggested by Gerbal's (1993, private communication) analysis of the Exosat X-ray images of many clusters, worsens the already illusory agreement between the observed and predicted tidal radii.

The Perseus cluster is not the only cluster showing a young dynamical age and claimed to be a prototype of evolved clusters: a ROSAT image of the Coma cluster shows that it has a many-peaked structure (White et al. 1993), pointing out that it is still forming. This hints that we may have overestimated the number of regular and virialized clusters or conversely that clusters are less evolved and more complex than they seem at first sight.

Incidentally, we note that the young age of the Perseus and Coma clusters does not favor a hot dark matter dominated universe, where the first structures to form are the larger ones (Faber 1983).

6.5. The morphology-density and morphology-radius relations

No morphology-density or morphology-radius relations are detected in the inner region of Perseus, or else they are detected at a very low statistical level. In the latter case, the detection is due to the presence of strong non-uniformities in the distribution of types which are located at different densities or clustercentric radii. This means that the primary source of morphological segregation in this cluster is tied to the morphological non-uniformities rather than to the local density or to the distance from the cluster center and that the latter relations, when present, are induced by these morphological non-uniformities.

We think that understanding the primary source of segregation in clusters is crucial. Is it necessarily a non-uniform distribution of types, for *all* clusters as for the inner region of Perseus, or can it be a morphology-density or a morphology-radius relation?

In this respect, previous studies of morphological segregation in clusters, based principally on catalogues of visually classified galaxies, are inconclusive for two possible reasons. First, the morphological misclassification present in all samples of visually classified galaxies strongly smoothes morphological non-uniformities; second, the method used to form artificial clusters by spatial superimposition of many clusters (Dressler 1980; Sanromà & Salvador-Solé 1990; Whitmore et al. 1993) erases all

[1] Even though we see the Perseus cluster in projection, it is likely to be morphologically non-uniform in the third dimension as well, at least if we are not in a privileged direction.

non radial non-uniformities (at least if there is not a privileged direction in the Universe) and consequently only leaves radial and density segregations.

In any case, our results on Perseus make clear that the morphology-radius or morphology-density relations do not *necessarily and immediately* imply that the local density or clustercentric distance play a fundamental role in determining the galaxy morphology, as previously suggested, since other possible and stronger relations could be responsible for the observed ones, as is the case for the inner region of Perseus.

The analysis of the Coma cluster, in progress, will help clarify this point.

Acknowledgements. I thank E. Davoust for having proposed this subject, for useful discussions and for carefully reading this paper at various stages. A particular acknowledgement goes to my future wife for her patience in staying so far away from me. I thank the anonymous referee for asking me to stress the main result of this work. This work was partially supported by grants from Torino University and the French Ministry of Foreign Affairs.

References

Andreon S., 1993, A&A, 276, L17
Bahcall N., 1974, ApJ 187, 439
Bahcall N., 1977, ApJ 218, L93
Baggett W., Anderson K., 1992, AJ 103, 436
Bautz L.P., Morgan W.W., 1970, ApJ, 162, L149
Beers T., Forman W., Huchra J., Jones C., Gebhardt K., 1991, AJ, 102, 1581
Bender R., 1988a, A&A 193, L7
Bender R., 1988b, A&A 202, L5
Bender R., Surma P., Döbereiner S., Möllenhoff C., Madejsky R., 1989, A&A 217, 35
Binggeli B., Tammann G., Sandage A., 1987, AJ 94, 251
Branduardi-Raymont G. et al., ApJ 248, 55
Bucknell M.J., Godwin J.G., Peach J.V., 1979, MNRAS 188, 579
Cavaliere A., Santangelo P., Tarquini G., Vittorio N., 1986, ApJ 305, 601
Contini T., Considère S., Davoust E., 1993, in preparation
Dressler A., 1980, ApJ 236, 351
Faber S., 1983, In Large-Scale Structure of the Universe, Cosmology and Fundamental Physics, First ESO-CERN Symposium, eds. G. Setti and L. Van Hove (CERN, Genevre)
Fasano G., 1991, MNRAS 24, 208
Forman W., Jones C., 1982, ARA&A 20, 547
Kendall M, Stuart A., 1948, The advanced theory of statistics, ed Griffin G. & Company Limited, London & High Wycombe
Kent S., Sargent W., 1983, AJ 88, 6
Kormendy J., 1977, ApJ 218, 333
Lauer T., 1988, ApJ 235, 49
Longo G., Capaccioli M., Bender R., Busarello G., 1989, A&A 225, L17
Melnick J., Sargent W., 1977, ApJ 215, 401
Merritt D., 1984, ApJ 276, 26
Nieto J.-L., 1988, in 2da Reunion de Astronomia Extragalactica, Academia nacional de Cencias de Cordoba, pag. 239
Nieto J.-L., Bender R., 1989, A&A 215, 266
Nieto J.-L., Bender R., Poulain P., Surma P., 1992, A&A 257, 97
Nieto J.-L., Bender R., Surma P., 1991, A&A, 244, L37
Nieto J.-L., Poulain P., Davoust E., Rosenblatt P., 1991, A&AS 88, 559
Nieto J.-L., Poulain P., Davoust E., 1993, A&A, in press
Oemler A., 1976, ApJ 209, 693
Ostriker J., Hausman M., 1977, ApJ 217, L125
Paturel G., Fouqué P., Bottinelli L., Gouguenheim L., 1989, Catalogue of Principal Galaxies, Observatoire de Lyon
Poulain P., Nieto J.-L., Davoust E. 1991, A&AS, 95, 129
Sanromà M.,Salvador-Solé E., 1990, ApJ 360, 16
Sarazin C., 1986, X-ray emission from clusters of galaxies, eds. R. Davies, J. Pringle and G. Efstathiou, Cambridge University Press
Schweizer F., Seitzer P., Faber S.M., Burstein D., Dalle Ore C.M., Gonzales J.J., 1990, ApJ 364, L33
Vettolani G., Gregorini L., 1988, A&A 189, 39
West M., Oemler A., Dekel A., 1988, ApJ 327, 1
White S. 1976, MNRAS 177, 717
White S., Briel U., Henry J.P. 1993, MNRAS 261, L8
Whitmore B., Gilmore D., Jones C. 1993, ApJ 407, 489

This article was processed by the author using Springer-Verlag TEX A&A macro package 1992.